3rd International Conference Advanced Mechanics: Structure, Materials, Tribology

Computational features of numerical solution of non–stationary wave problems for an underground pipeline under seismic impacts

AIPCP25-CF-AMSMT2025-00040 | Article

Computational features of numerical solution of non–stationary wave problems for an underground pipeline under seismic impacts

Karim Sultanov[1, a)], Sabida Ismoilova[1], and Nodirbek Akbarov[1]

[1]*Institute of Mechanics and Seismic Stability of Structures named after M.T. Urazbaev, Uzbekistan Academy of Sciences, Tashkent, Uzbekistan*

[a)] Corresponding author: sultanov.karim@mail.ru

Abstract. This article explores one–dimensional, nonstationary nonlinear wave problems involving an underground pipeline and the surrounding soil medium. The two systems are interconnected through conditions at their contact surface. Nonlinear laws that describe the variation of the friction force, which occurs in two stages, govern these conditions. In the initial stage, the friction force develops in response to relative displacement. In the second stage, the friction behavior conforms to the Amontons–Coulomb law. The numerical solution to this problem was obtained by employing the method of characteristics, followed by the finite difference method. During the process of obtaining numerical solutions, it was observed that the discretization steps in the computational domains on two conjugate characteristic planes significantly influence the stability of the results. This article discusses these computational features and other important aspects relevant to achieving a stable numerical solution for the "underground pipeline–soil medium" mechanical system. By establishing appropriate discretization steps, stable numerical solutions were successfully derived for the wave problems in question. The analysis of the numerical results indicated that when a low–frequency seismic wave propagates in soil, it generates soliton–like interaction waves with large amplitudes in the underground pipeline.

INTRODUCTION

The challenges associated with the seismic resistance of underground pipelines are often simplified to one–dimensional models [1–4]. In references [1] and [2], the pipeline is treated as a one–dimensional extended rod, which simplifies the analysis of its seismic resilience. References [3] and [4] consider the pipeline in conjunction with the surrounding soil medium, where the wave propagation problems for both the pipeline and the soil are addressed separately.

Non–stationary boundary value problems related to seismic wave propagation in soils are discussed in [5]. When a pipeline is situated within a soil medium experiencing a seismic load, the significantly greater deformation properties of the soil compared to those of the pipeline result in interaction forces at their contact surface. The longitudinal interaction laws between an underground pipeline and the surrounding soil are explored in [6], highlighting their notable nonlinearity due to the degradation of the soil contact layer under intense interaction [7]. The relevance of these laws to seismic resistance problems for underground pipelines is demonstrated in [4] and [7].

However, incorporating the external soil medium into the seismic resistance analysis for underground pipelines introduces complex coupled wave problems. This approach necessitates the simultaneous exploration of numerical solutions in two domains and their synchronization. This article focuses on the challenges of algorithm development and the achievement of stable numerical solutions for such non–stationary one–dimensional coupled nonlinear wave problems.

Numerous studies have been devoted to the wave processes in soils and numerical methods for solving wave problems for soils and underground pipelines were developed. The classical foundations of numerical methods and their practical application are presented in [8].

The three–dimensional numerical manifold method (3DNMM) has been further refined for mathematical modeling of wave propagation through homogeneous jointed rock masses, as discussed in [9]. To minimize the

negative impact of artificial boundaries, a viscous non–reflecting boundary is introduced to effectively absorb wave energy, thus enhancing the 3DNMM. Additionally, to model the elastic recovery properties of the infinite problem domain, a viscoelastic boundary, which evolves from the viscous non–reflecting boundary, is applied to improve the 3DNMM model.

Reference [10] focuses on a numerical method for computer modeling of wave propagation in three–dimensional dynamic loading problems for complex structures. This method utilizes a grid–characteristic approach that employs unstructured tetrahedral hierarchical meshes, multiple time steps, and high–order interpolation. By allowing the use of multiple time steps, the grid–characteristic method enhances performance and significantly reduces computation time.

In [11], an efficient method for modeling elastic wave propagation in unbounded domains is developed. It applies to soil–structure interaction problems involving scalar and vector waves, unbounded domains of arbitrary geometry, and anisotropic soil. A scalable boundary finite element method is used to derive a new equation for the unit impulse response matrix of displacement at the soil–structure interface. The proposed method is based on a piecewise linear approximation of the first derivative of the unit impulse response matrix of displacement and on the introduction of an extrapolation parameter to improve numerical stability. When combined, these two ideas allow the selection of significantly larger time steps compared to conventional methods, thus leading to higher efficiency.

In reference [12], the study aims to develop an efficient finite–difference scheme for solving direct seismic problems based on the equations governing the dynamics of elastic media in an axisymmetric formulation. For the numerical implementation of the scheme on multiprocessor computing systems, a two–cycle splitting method with respect to spatial variables was employed. During the splitting stages, one–dimensional systems of equations were decomposed into subsystems representing longitudinal, transverse, and torsional waves. This paper focused specifically on the case of longitudinal waves. A comparison was made between explicit grid–characteristic schemes and implicit predictor–corrector schemes with controlled energy dissipation, using exact solutions that describe traveling monochromatic waves.

In reference [13], traveling–wave solutions to the combined Korteweg–de Vries equation and a complex–coupled equation were obtained using the automatic Bäcklund transform method. The finite–difference method was utilized for the numerical approximation of the exact solutions. Additionally, these exact traveling–wave solutions were compared with the numerical solutions through tables and figures.

In reference [14], the Rayleigh wave velocity, a crucial parameter in ground motion analysis, was directly determined in an unconfined soil medium using numerical simulations with ABAQUS. The Rayleigh wave (R–wave) velocity was calculated from the displacement time history of a finite element model. Based on the results, a linear prediction equation for determining the R–wave velocity in soil was proposed. For this purpose, a two–dimensional finite element model was developed in conjunction with infinite elements at the boundary, subjected to dynamic loading. After confirming the presence of an R–wave in the soil medium through particle motion and verifying the displacement time history with analytical models, the R–wave velocity was determined using the positive peak vertical displacement of the particle.

Mathematical modeling of wave processes in soils is closely linked to examining how waves interact with structures within a soil medium. One of the most significant types of underground structures is trunk pipelines. A study referenced as [15] investigated the impact of dynamic behavior and lateral soil pressure on the dynamics of box culverts buried in dry, non–cohesive soils through numerical methods. This research explored how relative flexibility affects the dynamic displacements of the structure by varying both the dynamic shear modulus of the non–cohesive soil and the structural characteristics of the models. The study investigated shear strains, horizontal accelerations, wall deformations, and lateral dynamic soil pressures at various points of the culvert through numerical analysis. The findings from this numerical analysis were validated against results from a previous study that utilized centrifuge modeling. It was observed that the deformation patterns of the numerical models of the culverts align well with the data obtained from the centrifuge tests. The analysis revealed that dynamic lateral pressures acting on the sidewalls increase as the wall flexibility coefficient decreases. For a rigid prototype, the dynamic force on the sidewalls of a box culvert can be as much as 2.8 times the lateral soil load at rest. In contrast, for a flexible prototype, this dynamic force is only 1.6 times the static soil load [15].

In [16], a mathematical model was developed to assess the impact of seismic blast waves on a rock mass, particularly during the excavation process, using the principles of dynamic elasticity theory. An original finite–difference computational scheme was created for the numerical solution of this boundary value problem, employing the finite–difference method. The application of the splitting method to address a two–dimensional boundary value problem reduced the task to solving one–dimensional spatial differential equations. Additionally, efficient computational software was developed to implement the resulting numerical algorithm. Numerical solutions for the model problem are presented in the context of an elliptical excavation shape.

In [17], the challenge of accounting for highly uneven topography, inhomogeneities, and singularities in the ground domain is addressed. This consideration is essential for solving a variety of seismic problems, such as determining the locations of earthquakes. Therefore, employing a grid method that allows for a nonuniform distribution of grid nodes may be beneficial for modeling these issues. The longstanding use of finite–difference methods in modeling seismic wave propagation has enabled researchers to tackle this problem effectively. To validate the results, a numerical model was created using FLAC geotechnical software.

The review article [18] discusses the perfectly matched layer (PML) method and its various formulations that have been developed over the past 25 years for numerical modeling and simulating wave propagation in unbounded media. To enhance computational efficiency, the proposed time–domain formulation of the PML employs a hybrid approach. This combines a mixed (displacement–deformation) formulation for the PML domain with a classical (displacement–based) formulation for the physical domain of interest. The methodology utilizes the standard Galerkin finite element method (FEM) for spatial discretization, alongside a Newmark time–domain scheme paired with a finite difference (Crank–Nicolson) scheme for temporal discretization.

A brief analysis of studies [19] on the seismic interaction between soils and structures indicates that wave processes in soils and underground pipelines are being extensively researched worldwide. Most of the problems addressed in the literature are solved using numerical methods based on developed complex mathematical models that describe both one–dimensional and multidimensional motions of media and bodies.

An analysis of references [20–22] suggests that developing mathematical models to understand wave propagation in soils and their interaction with underground structures is a crucial first step. When dealing with nonlinear models, challenges may arise in obtaining accurate solutions to the problems being studied. Since numerical solutions are approximate, it is crucial to conduct thorough numerical experiments to ensure that the answers to these questions are reliable. Therefore, when constructing mathematical models and numerical solution algorithms, it is essential to consider all the specific features that may impact the results.

PROBLEM STATEMENT AND SOLUTION METHOD

The general problem of wave propagation in a soil medium, including an underground pipeline, is three–dimensional. However, solving such a problem numerically can lead to significant mathematical challenges. Therefore, as proposed in sources [1–3], we will use a simplified calculation method. In this approach, the soil and underground pipeline are modeled as a coaxial composite rod system, consisting of two layers along the radius.

In this model, the outer hollow rod represents the soil medium, while the inner rod represents the pipeline. Since we are focusing on a trunk pipeline, we assume its length is sufficiently large from the initial cross–section $x = 0$. The initial cross–section ($x = 0$, where x is the pipeline axis) is assumed to be a fixed cross–section of the soil and pipeline, where the seismic wave in the soil is set.

This calculation scheme significantly simplifies the original three–dimensional problem, reducing it to a one–dimensional model. This simplification, which is effective in studies [4, 20], retains the fundamental characteristics and essence of the wave propagation process within both the soil and the pipeline, despite the reduction in complexity.

This article examines a non–stationary wave process in a soil medium and an underground pipeline. While most studies on the seismic resistance of underground pipelines focus on stationary vibrations under seismic loads, it is well–known that during earthquakes, the vibrations of both buildings and structures, as well as underground pipelines, are non–stationary. Therefore, understanding the initial stages of underground pipeline vibrations under seismic loads is of significant interest. In light of this, the article poses and solves non–stationary boundary value problems related to the processes being considered.

The deformation laws for the soil and pipeline are assumed to be linear viscoelastic (a standard linear body):

$$\frac{d\varepsilon_i}{\mathrm{dt}} + \mu_i \varepsilon_i = \frac{d\sigma_i}{E_{\mathrm{Di}}\mathrm{dt}} + \mu \frac{d\sigma_i}{\mathrm{iE_{Si}}}$$
$$\mu_i = E_{\mathrm{Di}}\, E_{\mathrm{Si}} / (E_{\mathrm{Di}} - E_{\mathrm{Si}})\eta_i \quad (1)$$

Here and below, i=1.2. For i=1, the parameter values refer to the pipeline, and for i=2, to the soil.

In (1), σ– is the longitudinal stress, ε– is the longitudinal strain, t – is time, E_S– is the static modulus of elasticity, E_D – is the dynamic modulus of elasticity, μ– is the bulk viscosity parameter, η– is the bulk viscosity coefficient.

In [6], interaction laws were developed based on serial experiments on the interaction of underground structure elements with soil. The most adequate of these is the law developed based on a standard linear body in the following form:

for $\sigma_N > \sigma_N$, $0 \le u \le u$:

$$\frac{d\tau}{K_{\mathrm{xD}}(\sigma_N, I_S)\mathrm{dt}} + \mu_S(\sigma_N, I_S, \dot{u})\frac{\tau}{K_{\mathrm{xS}}(\sigma_N, I_S)} = \frac{\mathrm{du}}{\mathrm{dt}} + \mu_S(\sigma_N, I_S, \dot{u})u \quad (2)$$

for $\sigma_N > \sigma_N$, $u > u$:

$$\tau = c + f\sigma_N \quad (3)$$

for, $\sigma_N \leq \sigma_N$:

$$\tau = 0 \quad (4)$$

where τ– is the interaction (friction) force, u– is the relative displacement, $u=u_g–u_c$, u_g– is the absolute soil displacement, u_c– is the absolute pipeline displacement; $u*$– is the critical value of the relative displacement, upon reaching which the soil contact layer is completely destroyed; K_{xD} – is the variable dynamic soil stiffness coefficient (as $\dot{u} \to \infty$); K_{xS} – is the variable static soil stiffness coefficient (as $\dot{u} \to 0$); μ_S – is the variable parameter of soil shear viscosity; $\dot{u}=du/dt$– is the rate of relative displacement of the pipeline and soil; $I_S=u/u*$ – is the parameter characterizing the structural destruction of the soil contact layer, $0 \leq I_S \leq 1$, for $I_S=0$ is the soil contact layer when contact bonds between the outer surface of the pipeline and the soil are intact, and for $I_S=1$, this bond is completely destroyed; f_v– is the coefficient of internal friction of the soil; σ_N– is the stress normal to the outer surface of the pipeline; $^{*}_{N}$– is the ultimate tensile strength of the soil (from here on, compressive stresses are taken to be positive).

Specific types of variable coefficients included in equations (2) and their physical justifications are given in [4, 6]. Note that the above interaction laws (2) – (4), with the corresponding constitutive relations given in [4, 6], are nonlinear laws of interaction between an underground pipeline and the surrounding soil.

The equations for the longitudinal motion of the pipeline and soil along the x–axis, coinciding with the pipeline axis, are of the following form:

$$\begin{gathered} \rho_{0\,i}\partial\, v_i/\partial\, t - \partial\, \sigma_i/\partial\, x + \chi_i\sigma_{\tau\, i} = 0 \\ \partial\, v_i/\partial\, x - \partial\, \varepsilon_i/\partial\, t = 0 \end{gathered} \quad (5)$$

where v_i– is the particle velocity (mass velocity); σ_i, ε_i – are longitudinal stresses and strains; ρ_{0i}– is the initial density; $\chi_i=sign(v)$– for the rod, and $\chi_i=–sign(v)$– for soil; $v = v_2$ – is the soil particle velocity; σ_τ – is the reduced friction force acting per unit length of the rod.

The values of σ_τ for the pipeline and soil are determined from the following relationship:

$$\sigma_{\tau\, i} = 4D_{\mathrm{Hi}}\,\tau/(\,D_{\mathrm{Hi}}^2 - D_{\mathrm{Bi}}^2) \quad (6)$$

where τ – is the friction force (shear stress), determined from equations (2)–(4); D_{Hi} – are the outer diameters, and D_{Bi} – are the inner diameters of the pipeline and soil.

The solution to the problem is reduced to integrating the nonlinear system (5), closed by equations (1), separately for the pipeline (i = 1, an internal problem) and separately for the soil (i = 2, an external problem). This system is coupled by nonlinear conditions on the contact surface between the pipeline and the soil, which determine the laws of variation of the interaction force (friction) τ according to equations (2)–(4).

Boundary conditions are at x = 0, the load is specified as a sinusoidal wave at the initial cross–section of soil:

$$\begin{gathered} \sigma = \sigma_{\max}\sin(\pi t/T), 0 \leq t \leq \theta \\ \sigma = 0, t > \theta \end{gathered} \quad (7)$$

where T– is the half–period of the load, θ – is the duration of the load, σ_{max} – is the amplitude of the load, and σ – is the longitudinal stress acting along the x–axis.

The conditions at the wave fronts in the soil and pipeline are initially set to zero. The initial conditions for the problems are also zero.

Equations (5), closed by equation (1), are hyperbolic. They have real characteristics and characteristic relations. Solutions can be derived using these characteristic relations, which are represented as ordinary differential equations.

The most widely used method for obtaining numerical solutions to the system of wave equations represented by equations (5) and (1) is the finite difference method [8].

The two systems of equations (1) for the soil and (5) for the pipeline are coupled systems that are solved separately. In reference [22], a method for numerically solving similar hyperbolic wave equations was developed using the theory of characteristics and the Hartree calculation scheme. This method reduces the system of wave equations to ordinary differential equations by employing the method of characteristics, after which the finite difference method is applied implicitly to numerically solve these ordinary differential equations.

COMPUTATIONAL FEATURES OF OBTAINING NUMERICAL SOLUTIONS

The discretization domains, according to the method given in reference [22], on the characteristic plane *t, x* for the soil medium and the pipeline are shown in Fig. 1.

The main difference between the calculation schemes for the pipeline and soil is the space step value Δx_c. The time step values Δt for the soil and the pipeline are the same and common. While the time steps Δt are the same for both calculation schemes, the space steps differ by the ratio of the longitudinal wave velocities:

$$\Delta x_g = \Delta x_c \, C_{\text{og}}/C_{\text{oc}} \tag{8}$$

In this case, the space step for the soil Δx_g, according to (8), is smaller by the ratio of the longitudinal wave velocities C_{0g} / C_{0c} .

In Fig. 1, the spatial step for the pipeline is three times larger than that for the soil.

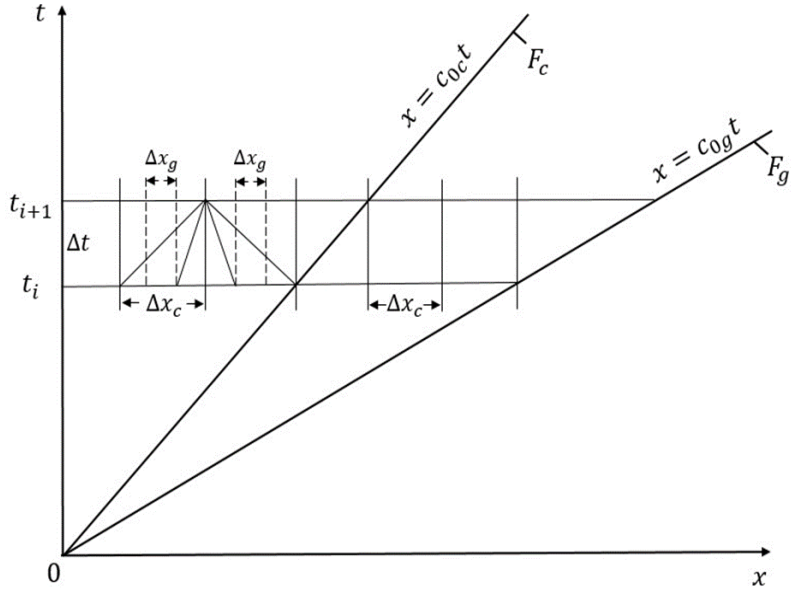

FIGURE 1. Domains of numerical solution for problems of wave propagation in soil and pipeline.

In Fig. 1, F_g– is the wave front in the soil; c_{0g}– is the longitudinal wave propagation velocity in the soil; Δx_g– is the discretization step in the soil along the *x*–axis; Δt– is the discretization step along the *t*–axis; t_{i+1} – is the upper, calculated time layer; t_i– is the lower, initial time layer; F_c – is the wave front in the pipeline; c_{0c} – is the longitudinal wave propagation velocity in the pipeline; Δx_c – is the discretization step along the x–axis for the pipeline.

Figure 1 shows two combined calculation schemes: the calculation schemes for the soil and the pipeline on the characteristic plane *t, x*. According to the Courant stability conditions, the characteristic must not extend beyond its cells for both the soil and the pipeline. This condition is satisfied here.

D.R. Hartree [22] proposed a calculation scheme illustrated in Fig. 1. The advantages of both the method of characteristics and the D.R. Hartree calculation scheme are discussed in detail in reference [22]. The core idea of this method is to seek the numerical solution within the fixed time layer t_{i+1}; the wave parameters in the time layer t_i are considered known. The spatial steps Δx_g and Δx_c are chosen such that the characteristic lines do not extend beyond the boundaries of a rectangular cell with sides Δt, Δx_g and Δt, Δx_c. The slope of the characteristic lines is determined by the wave propagation velocity in the soil and the pipeline.

The computational domain consists of the ordinate axis, where $x=0$, on one side, and the wave fronts in the pipeline F_c and soil F_g, on the other. This domain expands indefinitely between these two lines. As time *t* and spatial coordinates x increase, the computational domain continues to grow. Consequently, the number of discrete points in the computational time layer t_{i+1} for the soil and pipeline also increases over time. This demand for computational resources is substantial, as it requires significant power to perform the calculations. To address this issue, two approaches are employed. First, after filling the numerical arrays for the time layer, a “discharge” process is carried out. This involves eliminating data associated with individual discrete points in the time layer, allowing for further

calculations to be performed with doubled time steps Δt, Δx_g and Δx_c. While this procedure helps manage resource usage, it does result in some reduction in accuracy. Moreover, a sudden increase in the sampling steps Δt, Δx_g, Δx_c may cause abrupt changes ("jumps") in the wave parameters.

To avoid these artificial "jumps", which can lead to a slight decrease in wave parameters, it is essential to perform calculations with constant steps Δt, Δx_g, Δx_c throughout the entire process. This approach requires considerable computational resources, including processing speed and RAM. Calculating low–frequency wave parameters can sometimes take several hours. Therefore, it is necessary to limit these calculations to a single period or half–period. This limitation is further complicated when conducting parallel calculations for both the soil and the pipeline.

Figure 2 shows the types of calculation points on the calculation layer t_i t_{i+1}, on parallel planes tx. At $t= t_i$, all wave parameters and friction values are known. Calculation models are provided for cases where the longitudinal seismic wave propagation velocity in the pipeline is $C_{0c}=5000$ *m/s*, and in the soil, it is $C_{0g}=1000$ *m/s*. In this case $K_c=C_{0g} / C_{0c}=2$. The wave velocity in the pipeline is five times greater than in the soil. Other values and ratios of wave velocities in the pipeline and soil are also possible.

We convert to dimensionless variables and parameters using the following relationships (here, all parameters and quantities refer to the pipeline; for simplicity, their subscripts are omitted):

$$x^0 = \mu\, x/c_0\ ;\ t^0 = \mu\, x\ ;\ \sigma^0 = \sigma/\sigma_{\max}\ ;\ v^0 = v/v_{\max}\ ;$$
$$\varepsilon^0 = \varepsilon/\varepsilon_{\max}\ ;\ v_{\max} = -\sigma_{\max}/c_0\,\rho_0\ ;\ \varepsilon_{\max} = \sigma_{\max}/E_D\ ; \quad (9)$$

Using dimensionless variables and parameters (9), equations (1)–(8) are non–dimensionalized. Then, the dimensionless time Δt^0 and space Δx_c^0 steps for the pipeline become equal.

To obtain reliable numerical results, the solution domain is discretized based on the Courant stability condition:

$$\Delta x^0/\Delta t^0 \le 1 \quad (10)$$

In equation (10), Δx^0 is the dimensionless spatial discretization step, and Δt^0 is the dimensionless time discretization step. In Fig. 2 and further on, for simplicity, the superscripts are omitted.

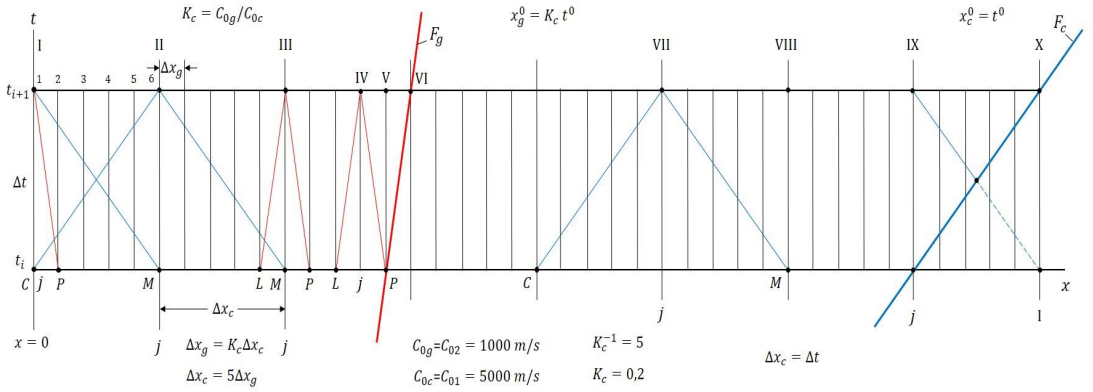

FIGURE 2. Typical discrete calculation points on the combined characteristic planes xt on the calculation time layer t_{i+1} t_i.

In Fig. 2, conditions (10) Δx_c /$\Delta t=1$ for the pipeline and Δx_g /$\Delta t=2$ for the soil ensure the stability of the numerical results.

In both cases, the characteristic lines do not extend beyond the computational cell with sides Δx_c , Δt for the pipeline and Δx_g , Δt for the soil.

When developing the algorithm for wave processes in the soil and pipelines, an important observation was made. The discretization step for the pipeline Δx_c is five times larger than that for the soil, Δx_g, i.e., Δx_c / $\Delta x_g=5$. Here, discrete point I at time t_{i+1} and point 1 coincide (Fig. 2). The next discrete points for the pipeline with the discretization step Δx_c, are points II, III…X. The wave parameters can be calculated separately for the pipeline and the soil, using the respective discretization steps. In this approach, the values of the wave parameters in the soil for points *P* and *L* are determined through linear interpolation between points *C* and *M*. Although this method significantly reduces computation time on the computer, it comes at the cost of degraded accuracy and stability, as will be demonstrated below.

Looking ahead, we observe that numerical experiments indicate that the wave parameters for the pipeline must also be determined at specific points in the soil, namely points 1, 2, 3, 4, 5, and 6, as illustrated in Fig. 2. In

numerical calculations, when we define the spatial step Δx_g for both the soil and the pipeline, the numerical solutions were found to be stable and smooth. However, this approach requires a significant amount of computational time.

Another issue arises when calculating the wave parameters in the pipeline at the initial points 2, 3, 4, and 5, which must be determined using a separate algorithm. At these discrete points, the left characteristic line for the pipeline extends beyond the initial cross–section $x=0$. To address this problem, we utilize a linear interpolation method. Specifically, the wave parameters in the pipeline for initial points 2, 3, 4, and 5, located between points I and II (as shown in Fig. 4), are determined through linear interpolation between discrete points 1 and 6. The calculation of the wave parameters in the pipeline using the general algorithm commences after the calculations at point 1, from point 6, or from point II (as shown in Fig. 2)

Therefore, numerical calculations of the wave parameters at time t_{i+1} for both the soil and the pipeline are modeled with the discrete spatial step Δx_g. The time step is taken $\Delta t= \Delta x_c =5\ \Delta x_g$ for $K_c=C_{0g} / C_{0l}$=0.2., and in other cases

$\Delta t= K_c^{-1}\Delta x_g$.

Calculations for discrete points of the pipeline using the above algorithm can be continued up to point III for the case where the points are arranged as in Fig. 2. Already at point III, the right characteristic line for the pipeline extends beyond the wave front line F_g. Calculations of the soil wave parameters can be carried out up to discrete point IV. At point V, the soil characteristic line already intersects the front line F_g in soil. Therefore, the soil wave parameters and interaction forces for point V are determined by linear interpolation between points IV and VI. Discrete point VI lies on the soil wave front, where all wave parameters are zero, since this front represents the lines of weak discontinuity.

Since the front line F_g is a weak discontinuity line, calculations of the wave parameters in the pipeline can be performed using a "through" calculation up to point VIII in Fig. 2. However, when the front line F_g is not a weak discontinuity line, this cannot be done. In this case, the wave parameters in the pipeline are also calculated taking into account the wave front in the soil. Calculations from point IX to point X are performed by interpolation. In this segment, the right–hand characteristic for the pipeline intersects the wave front line F_g in the pipeline. After the wave front F_g propagates in the pipeline, all soil particles are practically at rest. The equations for the wave front lines in the soil and the pipeline in dimensionless form are $\Delta x_g =K_c t$ and $\Delta x_c=t$, respectively.

Another feature of the algorithm is the calculation of points between the fronts F_g and F_c. It is important to note that the longitudinal seismic wave acts only in the soil and is initiated by the wave load at section x=0. This load does not act at this section of the pipeline, i.e., the initial section of the pipeline is load–free. A wave in the pipeline is generated solely by the interaction force (friction) that arises at the interface between the pipeline and the soil, specifically at the soil contact layer. Because the soil deforms more significantly than the pipeline, the friction force in the pipeline section from x=0 to the wave front F_g in the soil acts as an active force, prompting the pipeline to move. As a result, this movement generates waves within the pipeline, leading to the development of stresses, strains, and other related effects.

Behind the wave front F_g, a wave propagates through the pipeline. For this wave, the frictional force acts as a drag force (passive force), since there is no movement in the soil. Therefore, the wave in the pipeline behind the front F_g is quite weak. This same wave can generate a corresponding wave in the soil. However, as the calculation results show, it is practically zero. Based on numerical experiments, it was established that the main wave in the pipeline occurs from the initial section x=0 to the wave front in the soil F_g. In sections F_g F_c, where the soil is undisturbed, as will be shown below, significant stresses and strains do not occur in the pipeline.

Thus, taking into account the above features, resolving equations, and, based on them, algorithms for calculating the parameters of waves in the soil and pipeline were developed.

Soil characteristics are:

γ_{0g}= 20 kN/m^3 – specific gravity of soil;

D_{Ng}= 3 m – nominal outer diameter of the soil cylinder;

D_{Bg} = 0.15 m – nominal inner diameter of the soil cylinder;

K_σ= 0.3 – lateral soil pressure coefficient;

$\gamma_g=\gamma_2=E_{Dg} / E_{Sg}$=2– dimensionless quantity;

C_{0g}= 1000 m/s – longitudinal wave propagation velocity in soil;

C_{gS} = 500 m/s – transverse wave propagation velocity in soil.

Steel pipeline characteristics are:

γ_{0c} = 78 kN/m^3 – specific gravity of the pipeline material;

D_{Nc} = 0.15 m – outer diameter of the pipeline;

D_{Bc} = 0.14 m – inner diameter of the pipeline;

$\gamma_c=\gamma_l=E_{Dc}/E_{Sc}$=1.02– dimensionless quantity;

C_{0c} =5000 m/s – longitudinal wave velocity in the pipeline;

H_l=1.425 m – laying depth of the pipeline in soil;

μ_c=10000 s^{-1} – steel viscosity parameter;

L_c =107 m – nominal pipeline length.

Characteristics of the soil contact layer and pipeline–soil interaction are:

f_v=0.3 – coefficient of internal friction of soil;

C_v =10 kN/m^2 – soil cohesion coefficient;

u_*=10–3 m – relative displacement value at which the interaction process transitions to the Coulomb friction stage;

α=1.5 – dimensionless coefficient in formula (9);

χ=0.1 – dimensionless exponent in formula (11);

$\gamma_{vN}=K_{xDN}/K_{xSN}$=2– dimensionless quantity;

$\gamma_{v*}=K^*_{xD}/K^*_{xS}$ =4– dimensionless quantity.

Load characteristics are:

σ_{max}=0.7 MPa – longitudinal wave amplitude;

T= 10 s – half–period of a low–frequency longitudinal wave;

θ= 100 s – conventional duration of a longitudinal wave;

f= 1/2T=0.05 s–1 – frequency of a longitudinal wave in soil.

With these initial data, the frequency of longitudinal seismic waves is f= 1/2T=0.05 s^{-1}. This is a low–frequency wave. However, computer implementation and obtaining a numerical solution encounter the greatest difficulties for low–frequency seismic waves.

The above initial data are basic. If they are subsequently changed, this is noted separately.

In addition to the above initial data, the most important parameters of the numerical solutions are the discretization steps Δt, Δx_g and Δx_c in the solution domain on the characteristic plane tx.

Naturally, the accuracy and stability of the numerical solutions depend on the value of these discretization steps. Based on the analysis of numerical solutions of wave problems on the propagation of longitudinal waves in soils [5], the dimensionless time step is Δt^0 = 0.1; 0.05, or 0.01. This corresponds for μ_c=104 s^{-1} to dimensional times $\Delta t = \Delta t^0/\mu_c$ =10–5 s; 5*10–6 s, and 10–6 s. Then, for one half–period of the wave T=10 s, which corresponds to dimensionless time t^0=105, the number of discrete points is $n=T/\Delta t$=106. For Δt^0=0.01, which in the dimensional case is Δt =10–6 s, and n=107 along the t–axis. For Δt^0= 0.05, Δt = 5*10–6; n=2*106.

In the spatial coordinate x, the discretization steps are Δx_c^0=0.01 and Δx_c^0=0.1 for Δt^0= 0.1. For Δt^0=0.01, Δx_g^0= 0.001 and Δx_g^0=0.01.

In dimensional values, they take the following values: Δx_c =0.05 m for Δx^0=0.1 and Δx_c =0.005 mm for Δx_c^0=0.01. In these cases, the number of discrete points along the t^0–axis and along the Δx_c^0–axis are the same and are n=106 for Δx^0=0.1 and n=107 for x_c^0=0.01, respectively.

During the action time T= 10 s, the half–period of a longitudinal seismic wave for x_c^0 = 0.1, the wave travels a dimensionless distance $x_c^0=\Delta x_c^0 \cdot n$=0.1·$10^6$=$10^5$ along the pipeline. In soil, it is $x_c^0=K_c \cdot t_0^0$=0.2·10^5=2·10^4. In dimensional values, they are x_c=50000 m and x_g=10000 m.

Thus, for dimensionless Δt = 0.1 and Δx_c = 0.1; Δx_g =0.01, the values of t^0=105; x_c^0=105 and x_g^0=2·10^4 are dimensionless.

If the dimensionless sampling steps are taken ten times smaller, i.e., Δt^0=0.01; x_c^0=0.01; x_g^0=0.001, the number of discrete points in the half–period of the seismic longitudinal wave reaches 107 points; 107 points in the pipeline, and n_g=2·10^7 of discrete points in the soil.

As noted above, pipeline calculations are performed using discrete points in the soil, and the number of computational points in the pipeline is also 2·10^7. These data demonstrate the resources required to perform numerical calculations of wave processes in the soil and pipeline on two superimposed parallel characteristic planes tx. The computational domains in plane tx expand during wave propagation, and the number of discrete points in the computational time layer t_{i+1} increases. Computational experiments have shown that the sampling steps Δt^0= 0.05; x_c^0= 0.01, and x_g^0= 0.01 are the most optimal. Increasing their values leads to instability of the numerical solution, while a decrease in their values yields good, consistent results. However, the latter case requires a significant amount of computation time (10–15 hours) on modern, high–performance computers.

Therefore, in the case of low–frequency seismic waves, computer calculations were limited to one half–period of the waves propagating in soil.

Let us consider the calculation results. In the first calculation option, the dimensionless discretization steps were $\Delta t^0 = 0.1$; $x_c^0 = 0.1$; $x_g^0 = 0.01$.

Figure 3 shows the time profile of a longitudinal seismic wave in soil for the first half–period. Since the wave is low frequency, it propagates without attenuation, i.e., the wave amplitude remains unchanged σ_g=0.7 MPa for all considered cross–sections x=0; 5; 10; 15; 20; 25, and 30m from the initial cross–section (curves 1–7). The curve of changes $\sigma_g(t)$ in these sections, practically lies on a single curve (Fig. 3).

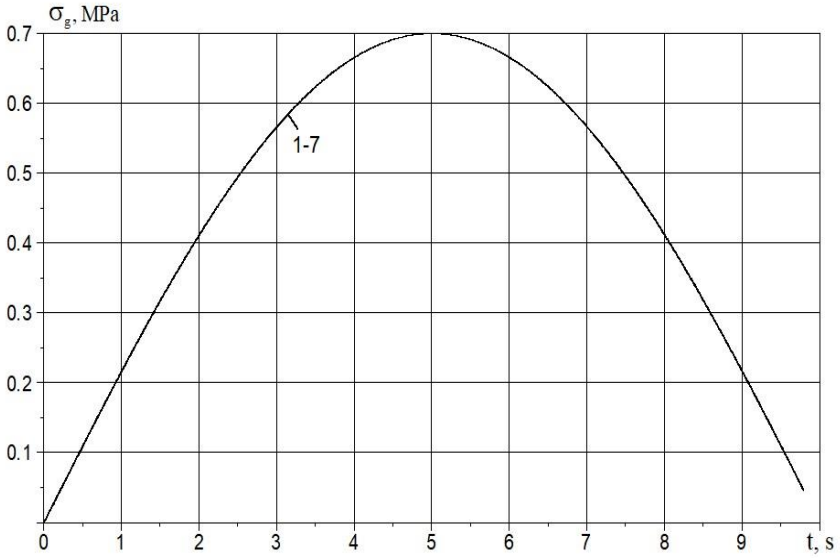

FIGURE 3. Half period of a seismic wave in soil with a frequency of f =0.05 s^{-1} at distances from the initial cross–section x= 0; 5; 10; 15; 20; 25; 30 m (curves 1–7)

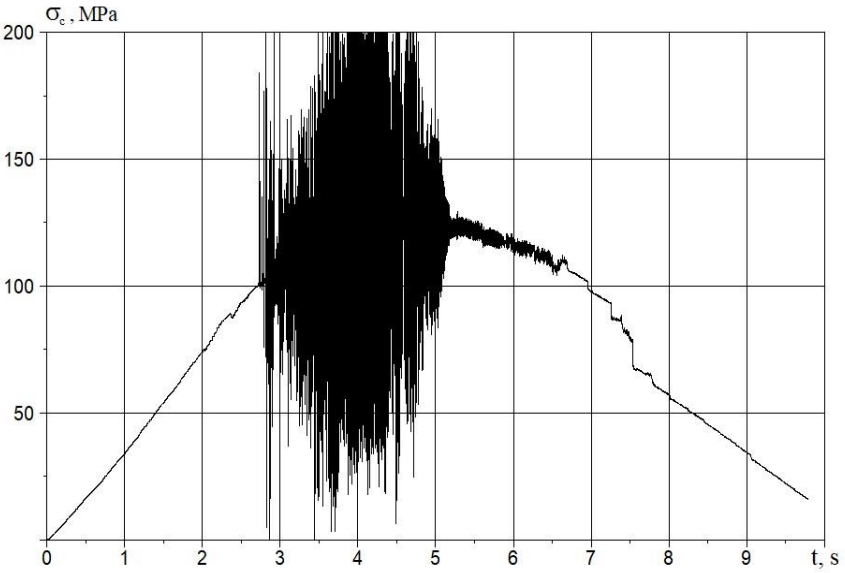

FIGURE 4. Changes in longitudinal stress over time in a pipeline at a cross–section of 5 m.

A completely different pattern is observed for a wave propagating along a pipeline. Figure 4 shows the wave profile over time for a pipeline cross–section of x=5 m. At the initial cross–section of the pipeline, x =0 m, according to boundary condition (7), no load is applied.

As seen from Fig. 7, the wave in the pipeline at x =5 m initially increases smoothly until x =2.8 sec. Then, strong instability in the stress value begins, lasting from 3 sec to 5 sec. The process then settles down again, and the stresses stabilize. The wave frequency remains virtually unchanged. The wave amplitude in the stability zones reaches
σ_c =125 MPa, which is significantly greater (by 178.6 times) than the wave amplitude in the soil (σ_g =0.7 MPa). This occurs due to the active behavior of the friction force at the pipeline–soil interface. In other words, the soil around the pipeline deforms significantly and “drags” the pipeline along with it, leading to the formation of high longitudinal stresses in the pipeline.

A similar pattern is observed at other cross–sections (x =10; 15; 20; 25, and 30 m) of the pipeline. Instability in longitudinal stress values in the pipeline occurs over time intervals from 3 sec to 5 sec. The amplitude of the wave in the pipeline decreases from σ_c =125 MPa at x =5 m to σ_c =115 MPa. In this case, the pipeline is considered elastic (γ_c =1.02), which prevents wave dissipation in the pipeline. Attenuation occurs due to the reduction in the active friction force on the outer surface of the pipeline.

The instability in stress values is linked to the variability of cross–sectional velocities within the pipeline. Figure 5 illustrates the changes in soil and pipeline cross–sectional velocities at x=0. The soil cross–sectional velocities vary smoothly from zero to a maximum of v_g =1.6 m/s and then gradually decrease (red curve in Fig. 5). This behavior can be attributed to the interaction force (an active frictional force), which has a negligible impact on the wave parameters in the soil. This is primarily due to the substantial nominal outer diameter of the soil (D_H=D_{Ng}=3 m), which is significantly larger by a factor of 20 than the outer diameter of the pipeline (D_H=D_{Nc}=0.15 m).

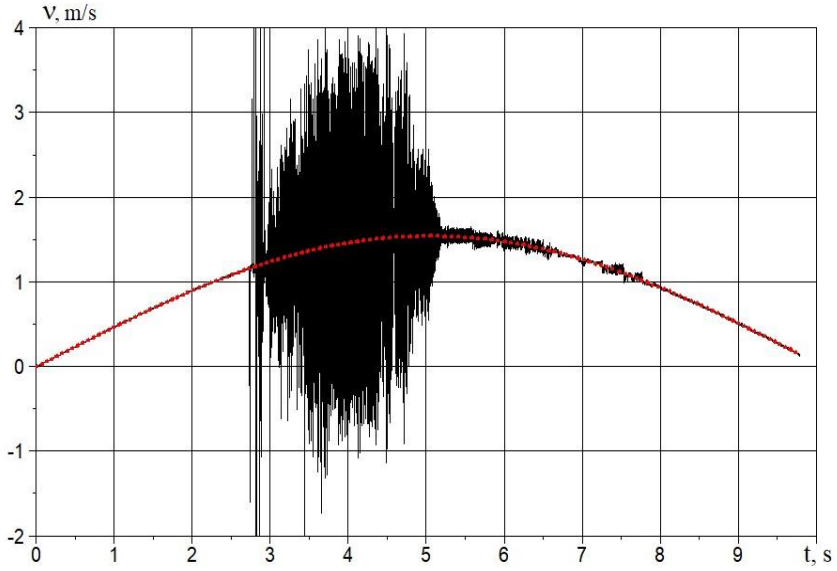

FIGURE 5. Changes in longitudinal cross–sectional velocities over time in the pipeline (black curve) and in the soil (red curve) at the initial cross–section x =0 m.

Instability in pipeline cross–sectional velocities, and consequently instability in relative velocities, leads to variability in shear stress values.

In [21], an exact analytical solution was obtained for the wave problem of shock wave propagation in embedded elastic rods, such as cages (holders). When the lengths of the rod and the cage (sleeve) are equal, as the wave propagates along them, after a certain time, the cross–sectional velocities of the rod and cage become equal. In [21], the rod and cage interact according to the Amontons–Coulomb law of dry friction.

In [20], a numerical solution was obtained for this problem in the case of viscoelastic rods and cages. Other laws of rod–cage interaction were also considered in [20]. In these cases, too, the velocities of the rod and cage cross sections become equal.

However, when solving these problems numerically, the velocities of the rod and cage cross–sections cannot be exactly equal. As a result, the relative velocity changes around zero with alternating signs. Consequently, the shear stress values also become alternating. As a result, we observe a loss of stability in the numerical solution results in the friction force values and dependencies, followed by a loss of stability in all other wave parameters of the underground pipeline.

In the second option, the discretization steps are Δt^0= 0.01; x_c^0= 0.01; x_g^0= 0.001. In this case, they are an order of magnitude smaller than in the first option.

The longitudinal stresses in the soil remain unchanged, as in Fig. 3. The changes in longitudinal stresses in the second option in the pipeline cross–sections at x = 5; 10; 15; 20; 25, and 30 m (curves 1–6) are shown in Fig. 6. All curves of changes in longitudinal stresses 1–6 practically overlap each other. The maximum stress value is σ_{1max} =112 MPa, which is approximately the same as the result of the first option (Fig. 4). However, the results of the second option show virtually no instability or stress bifurcation.

Figure 7 shows the changes in the velocity of pipeline sections over time at x =0; 5; 10; 15; 20; 25, and 30 m (curves 1–7). The amplitude of the velocity change is virtually identical to the result of the first option in Fig. 5. The results of the second method show no instability.

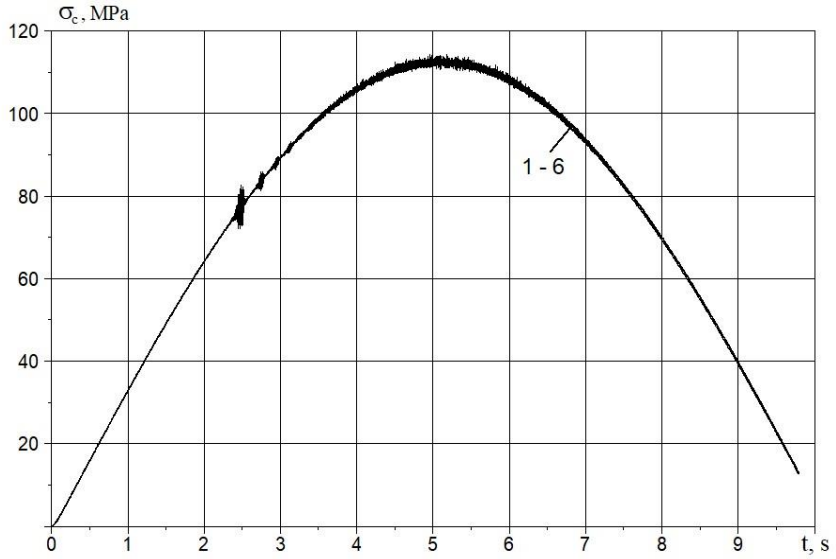

FIGURE 6. Changes in longitudinal cross–sectional velocities over time in the pipeline (black curve) and in the soil (red curve) at the initial cross–section x =0 m.

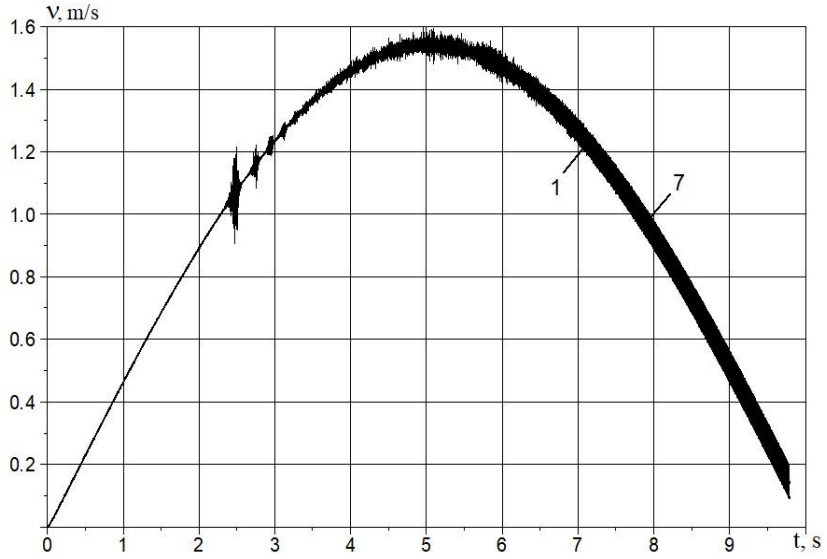

FIGURE 7. Velocity changes over time in pipeline cross–sections at x = 0; 5; 10; 15; 20; 25, and 30 m (curves 1–7).

However, note that as the seismic wave amplitude in the soil decreases, for example, at σ_{max} = 0.35 MPa, the instability of the wave parameters in the pipeline increases.

In the third option, calculations were performed with discrete steps x_c^0= 0.01; x_g^0= 0.01; Δt^0= 0.05. The amplitude of the longitudinal seismic wave in the soil was taken in dimensional form σ_{max} =0.35 MPa.

The values of other initial parameters remained unchanged.

In this case, the pattern of change in the longitudinal stress wave in the soil over time is similar to the one in Fig. 3, with the only difference being that the stress amplitude is σ_{gmax} =0.35 MPa.

Changes in longitudinal stresses in pipeline cross–sections at x=0; 5; 10; 15; 20; 25, and 30 m (curves 1–7) are shown in Fig. 8.

As can be seen from Fig. 8, the resulting numerical dependences $\sigma_c(t)$ are completely smooth, and no instability or bifurcations are observed.

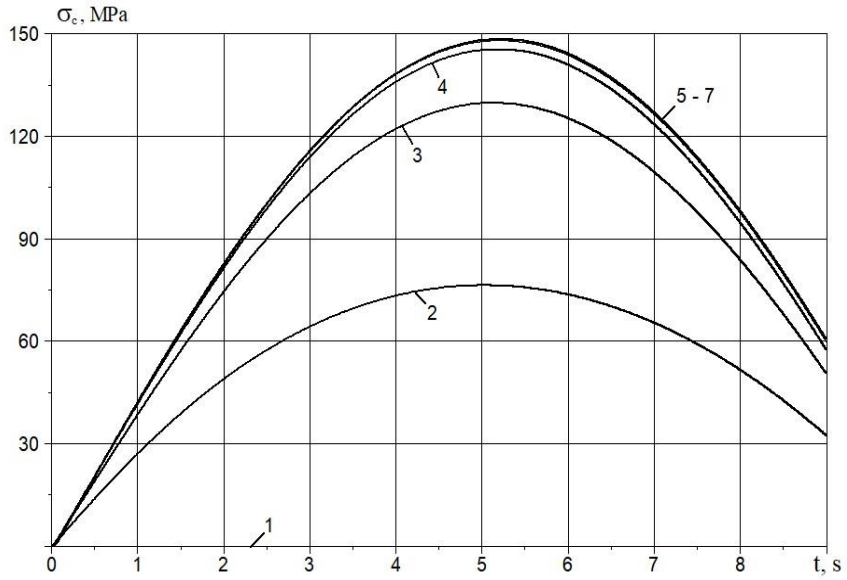

FIGURE 8. Changes in longitudinal stresses over time in pipeline cross–sections at x = 5; 10; 15; 20; 25 and 30 m (curves 1–7).

The longitudinal stress in the pipeline reaches the maximum σ_{cmax} =148.2 MPa. This value exceeds the amplitude of the longitudinal stress in the soil (σ_{gmax} =0.35 MPa) by 423.4 times. This multiple excess is the result of the active frictional force (interaction) acting on the underground pipeline due to soil deformation in the longitudinal direction (along the pipeline axis). This maximum stress is reached gradually along the pipeline. At the initial cross–section of the pipeline, the load is unaffected, and the stress values are zero (line 1). At the next pipeline cross–sections at x= 5 m and 10 m (curves 2 and 3), the stress amplitude gradually increases and at x = 15 m, it practically reaches its maximum σ_{cmax} =148.2 MPa (curve 4). Further, in the pipeline cross–sections at x = 20, 25, and 30 meters, this stress amplitude σ_{cmax} = 148.2 MPa remains constant. A powerful wave with a high amplitude travels along the pipeline. Calculations indicate that the wave's propagation velocity along the pipeline is significantly lower than the speed of sound within it. This leads to the discovery of a new, soliton–like interaction wave that moves at a different velocity compared to conventional longitudinal waves in the absence of surrounding soil. The investigation of this wave's properties falls outside the scope of this study and will be addressed in future research.

Figure 9 shows the changes in (longitudinal) strains over time in the soil (curves 1^0–7^0) and the pipeline (curves 1–7) at x = 0; 5; 10; 15; 20; 25, and 30 m, respectively.

As can be seen from Fig. 9, the longitudinal strains in all soil sections are identical (curves 1^0–7^0). In the pipeline, these strains, like the stresses, gradually increase until they reach an asymptotic value, which then remains constant. Notably, the maximum longitudinal strain in the pipeline (amplitude) is more than double the strain amplitude observed in the soil.

It is known that the quasi–static theory of seismic resistance of underground pipelines [1, 20] is based on the hypothesis of equality of soil and pipeline strains under seismic impacts. As seen from Fig. 9, this hypothesis is not fulfilled. Nevertheless, the quasi–static theory is currently used as a basis for normative methods [20].

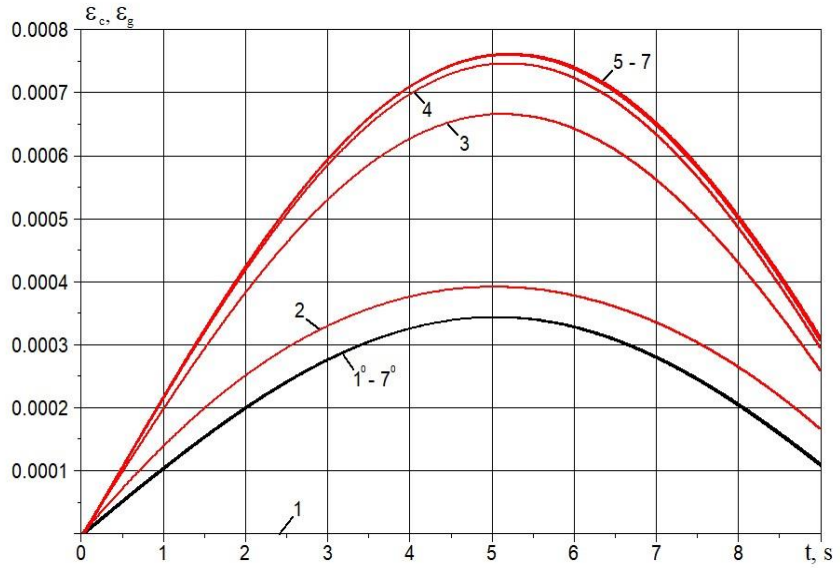

FIGURE 9. Changes in soil strains (curves 1^0–7^0) and pipeline (curves 1–7) over time at x = 0; 5; 10; 15; 20; 25, and 30 m.

Figure 10 shows changes in the velocity of soil particles (curves 1^0–7^0) and pipeline cross–sections (curves 1–7) over time at x= 0; 5; 10; 15; 20; 25, and 30 m. As seen from Fig. 10, the velocities of soil particles and pipeline cross–sections are almost identical. According to the changes in the relative velocity of the soil and pipeline v_t (Fig. 11), at x = 0, the maximum value of the relative velocity is v_{tmax} = 0.0021 m/s (curve 1). At x = 5 m, the values are v_{tmax} = 0.0004 m/s (curve 2), and at x = 10 m, v_{tmax} = 0.0002 m/s. In the remaining sections at x = 15 m; 20 m; 25 and 30 m (curves 4–7), the values of the relative velocity are practically zero.

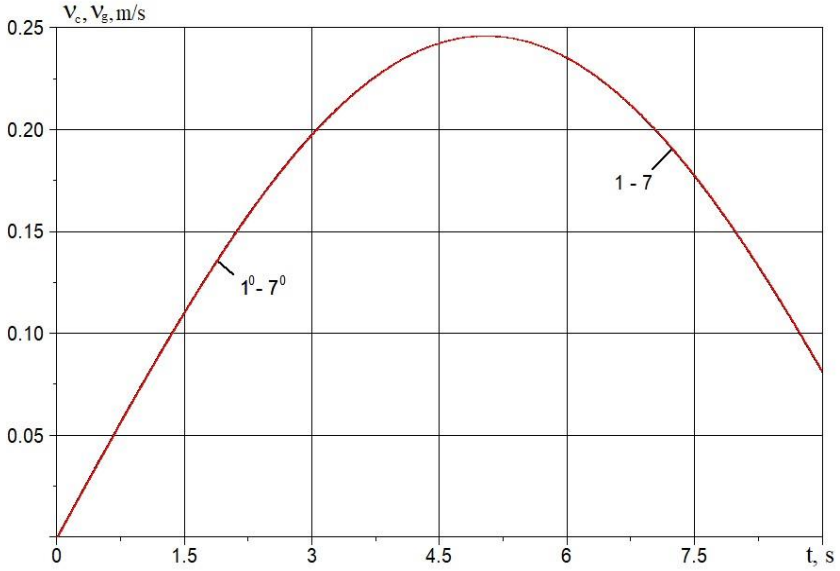

FIGURE 10. Changes in soil particle velocity (curves 1^0–7^0) and pipeline velocity (curves 1–7) over time in cross–sections at x = 0; 5; 10; 15; 20; 25, and 30 m.

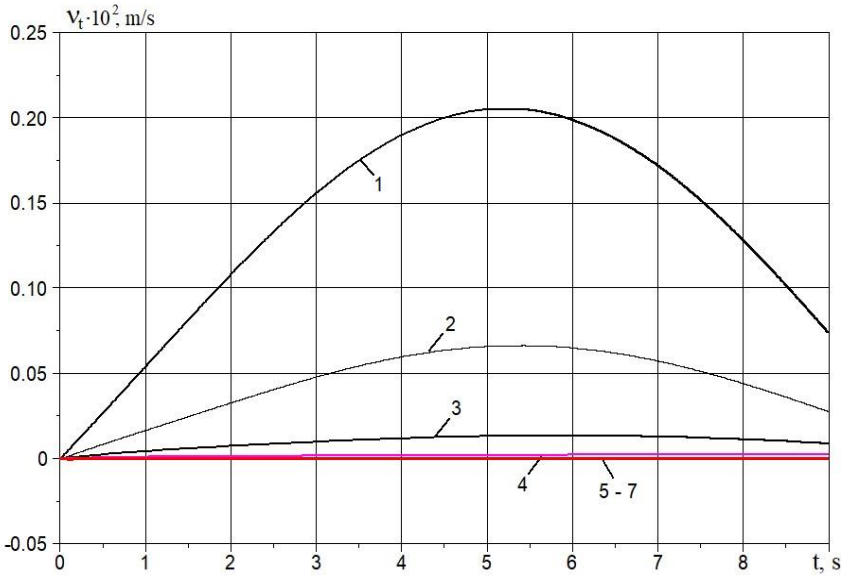

FIGURE 11. Changes in relative velocity over time in pipeline cross–sections at x = 0; 5; 10; 15; 20; 25, and 30 m (curves 1–7).

These results confirm that the soil and pipeline velocities ultimately become equal, as in [21].

CONCLUSIONS

The study focuses on the wave propagation process in a soil medium that contains an embedded underground pipeline, considering their interaction. Equations for the wave processes occurring in both the soil and the pipeline are defined and derived. Based on these equations, we develop an algorithm to numerically solve the wave problems using the method of characteristics and the finite difference method with an implicit calculation scheme.

The features of the developed numerical solution algorithm and methods to overcome them are determined. Based on the developed algorithm, a program for numerically solving the wave problems was developed in the FORTRAN–2005 algorithmic language. The program was implemented on a computer, and numerical experiments were used to determine the stability and reliability conditions for the resulting numerical solutions.

By conducting numerical experiments and analyzing the numerical solutions, the optimal discretization steps were determined in the solution domain on the characteristic plane tx for the soil medium and the underground pipeline.

It has been established for the first time that an active interaction force, specifically friction, can generate a soliton–like wave in an underground pipeline. This wave propagates through the pipeline without attenuation at a velocity lower than the speed of sound in the material of the pipeline.

Numerical calculations indicate that the assumption of equal longitudinal strains in both the soil and the pipeline, which underpins the standard quasi–static theory of underground pipelines, is not valid under the longitudinal action of a seismic wave.

ACKNOWLEDGMENTS

The work was conducted at the expense of the grant AL–8924073446 of the Agency for Innovative Development under the Ministry of Higher Education, Science, and Innovation of the Republic of Uzbekistan.

REFERENCES

1. M. J. O'Rourke and X. Liu, *Response of Buried Pipelines Subject to Earthquake Effects* (MCEER, Univ. at Buffalo, USA, 1999).

2. T. D. O'Rourke, J. K. Jung, and C. Argyrou, *Soil Dyn. Earthq. Eng.* **91**, 272–283 (2016). https://doi.org/10.1016/j.soildyn.2016.09.008
3. M. S. Israilov, *Mech. Solids* **58**, 26–37 (2023). https://doi.org/10.31857/S0572329922060083
4. K. S. Sultanov, *Facta Univ. Ser. Mech. Eng.* **22**, 485–501 (2024). https://doi.org/10.22190/FUME231227017S
5. K. S. Sultanov, *J. Appl. Math. Mech.* **66**, 115–122 (2002). https://doi.org/10.1016/S0021-8928(02)00015-1
6. K. S. Sultanov, *Int. Appl. Mech.* **29**, 217–223 (1993). https://doi.org/10.1007/BF00847001
7. A. A. Bakhodirov, S. I. Ismailova, and K. S. Sultanov, *J. Appl. Math. Mech.* **79**, 587–595 (2015). https://doi.org/10.1016/j.jappmathmech.2016.04.005
8. B. Alder, S. Fernbach, and V. Rotenberg, *Methods in Computational Physics*, Vol. 3 (Academic Press, New York and London, 1964).
9. Y. Yang, J. Li, and W. Wu, *Sci. China Tech. Sci.* **67**, 835–852 (2024). https://doi.org/10.1007/s11431-023-2517-8
10. I. B. Petrov, A. V. Favorskaya, N. I. Khokhlov, V. A. Miryakha, A. V. Sannikov, K. A. Beklemysheva, and V. I. Golubev, Radioelectron. Nanosyst. Inf. Technol. 7, 34 (2015). https://doi.org/10.17725/rensit.2015.07.034
11. X. Chen, C. Birk, and C. Song, Soil Dyn. Earthq. Eng. 65, 243–255 (2014). https://doi.org/10.1016/j.soildyn.2014.06.019
12. V. M. Sadovskii, O. V. Efimov, and E. A. Efimov, *J. Sib. Fed. Univ. Math. Phys.* **13**, 644–654 (2020). https://doi.org/10.17516/1997-1397-2020-13-5-644-654
13. A. Yokuş and D. Kaya, *Int. J. Mod. Phys. B* **34**, 2050282 (2020). https://doi.org/10.1142/S0217979220502823
14. K. S. Beena and M. N. Sandeep, *Indian Geotech. J.* (2021). https://doi.org/10.1007/s40098-021-00530-x
15. O. L. Ertugrul, *KSCE J. Civ. Eng.* **20**, 1737–1746 (2016). https://doi.org/10.1007/s12205-015-0235-1
16. A. P. Gospodarikov, Y. N. Vykhodtsev, and M. A. Zatsepin, *J. Min. Inst.* **224**, 405–414 (2017). https://doi.org/10.25515/pmi.2017.4.405
17. J. J. Benito, F. Ureña, E. Salete, A. Muelas, L. Gavete, and R. Galindo, *Soil Dyn. Earthq. Eng.* **79**, 190–198 (2015). https://doi.org/10.1016/j.soildyn.2015.09.012
18. F. Pled and C. Desceliers, *Arch. Comput. Methods Eng.* **29**, 471–518 (2022). https://doi.org/10.1007/s11831-021-09581-y
19. V. Anand and S. R. Satish Kumar, *Structures* **16**, 317–326 (2018). https://doi.org/10.1016/j.istruc.2018.10.009
20. K. S. Sultanov and N. I. Vatin, *Appl. Sci.* **11**, 1797 (2021). https://doi.org/10.3390/app11041797
21. L. V. Nikitin, *Statics and Dynamics of Rigid Bodies with External Friction* (Moscow Lyceum Publishing House, Moscow, 1998), 272 p.
22. N. E. Hoskin, in *Methods in Computational Physics*, Vol. 3, edited by B. Alder, S. Fernbach, and M. Rotenberg (Academic Press, New York and London, 1964), pp. 265–293.

LICENSE TO PUBLISH AGREEMENT FOR CONFERENCE PROCEEDINGS

This License to Publish must be signed and returned to the Proceedings Editor before the manuscript can be published. If you have questions about how to submit the form, please contact the AIP Publishing Conference Proceedings office (confproc@aip.org). For questions regarding the copyright terms and conditions of this License, please contact AIP Publishing's Office of Rights and Permissions, 1305 Walt Whitman Road, Suite 300, Melville, NY 11747-4300 USA; Phone 516-576-2268; Email: rights@aip.org.

Article Title ("Work"): Computational features of numerical solution of non-stationary wave problems for an underground pipeline under seismic impacts

(Please indicate the final title of the Work. Any substantive changes made to the title after acceptance of the Work may require the completion of a new agreement.)

All Author(s): Karim Sultanov, Sabida Ismoilova and Nodirbek Akbarov

(Please list **all** the authors' names in order as they will appear in the Work. All listed authors must be fully deserving of authorship and no such authors should be omitted. For large groups of authors, attach a separate list to this form.)

Title of Conference: International Conference Advanced Mechanics Structure Materials, Tribology

Name(s) of Editor(s) Prof. Dr. Valentin L. Popov

All Copyright Owner(s), if not Author(s):

(Please list **all** copyright owner(s) by name. In the case of a Work Made for Hire, the employer(s) or commissioning party(ies) are the copyright owner(s). For large groups of copyright owners, attach a separate list to this form.)

Copyright Ownership and Grant of Rights

For the purposes of this License, the "Work" consists of all content within the article itself and made available as part of the article, including but not limited to the abstract, tables, figures, graphs, images, and multimedia files, as well as any subsequent errata. "Supplementary Material" consists of material that is associated with the article but linked to or accessed separately (available electronically only), including but not limited to data sets and any additional files.

This Agreement is an Exclusive License to Publish not a Transfer of Copyright. Copyright to the Work remains with the Author(s) or, in the case of a Work Made for Hire, with the Author(s)' employer(s). AIP Publishing LLC shall own and have the right to register in its name the copyright to the proceedings issue or any other collective work in which the Work is included. Any rights granted under this License are contingent upon acceptance of the Work for publication by AIP Publishing. If for any reason and at its own discretion AIP Publishing decides not to publish the Work, this License is considered void.

Each Copyright Owner hereby grants to AIP Publishing LLC the following irrevocable rights for the full term of United States and foreign copyrights (including any extensions):

1. The exclusive right and license to publish, reproduce, distribute, transmit, display, store, translate, edit, adapt, and create derivative works from the Work (in whole or in part) throughout the world in all formats and media whether now known or later developed, and the nonexclusive right and license to do the same with the Supplementary Material.
2. The right for AIP Publishing to freely transfer and/or sublicense any or all of the exclusive rights listed in #1 above. Sublicensing includes the right to authorize requests for reuse of the Work by third parties.
3. The right for AIP Publishing to take whatever steps it considers necessary to protect and enforce, at its own expense, the exclusive rights granted herein against third parties.

Author Rights and Permitted Uses

Subject to the rights herein granted to AIP Publishing, each Copyright Owner retains ownership of copyright and all other proprietary rights such as patent rights in the Work.

Each Copyright Owner retains the following nonexclusive rights to use the Work, without obtaining permission from AIP Publishing, in keeping with professional publication ethics and provided clear credit is given to its first publication in an AIP Publishing proceeding. Any reuse must include a full credit line acknowledging AIP Publishing's publication and a link to the Version of Record (VOR) on AIP Publishing's site.

Each Copyright Owner may:

1. Reprint portions of the Work (excerpts, figures, tables) in future works created by the Author, in keeping with professional publication ethics.
2. Post the Accepted Manuscript (AM) to their personal web page or their employer's web page immediately after acceptance by AIP Publishing.
3. Deposit the AM in an institutional or funder-designated repository immediately after acceptance by AIP Publishing.
4. Use the AM for posting within scientific collaboration networks (SCNs). For a detailed description of our policy on posting to SCNs, please see our Web Posting Guidelines (https://publishing.aip.org/authors/web-posting-guidelines).
5. Reprint the Version of Record (VOR) in print collections written by the Author, or in the Author's thesis or dissertation. It is understood and agreed that the thesis or dissertation may be made available electronically on the university's site or in its repository and that copies may be offered for sale on demand.
6. Reproduce copies of the VOR for courses taught by the Author or offered at the institution where the Author is employed, provided no fee is charged for access to the Work.
7. Use the VOR for internal training and noncommercial business purposes by the Author's employer.
8. Use the VOR in oral presentations made by the Author, such as at conferences, meetings, seminars, etc., provided those receiving copies are informed that they may not further copy or distribute the Work.
9. Distribute the VOR to colleagues for noncommercial scholarly use, provided those receiving copies are informed that they may not further copy or distribute the Work.
10. Post the VOR to their personal web page or their employer's web page 12 months after publication by AIP Publishing.
11. Deposit the VOR in an institutional or funder-designated repository 12 months after publication by AIP Publishing.
12. Update a prior posting with the VOR on a noncommercial server such as arXiv, 12 months after publication by AIP Publishing.

Author Warranties

Each Author and Copyright Owner represents and warrants to AIP Publishing the following:

1. The Work is the original independent creation of each Author and does not infringe any copyright or violate any other right of any third party.
2. The Work has not been previously published and is not being considered for publication elsewhere in any form, except as a preprint on a noncommercial server such as arXiv, or in a thesis or dissertation.
3. Written permission has been obtained for any material used from other sources and copies of the permission grants have been supplied to AIP Publishing to be included in the manuscript file.
4. All third-party material for which permission has been obtained has been properly credited within the manuscript.
5. In the event that the Author is subject to university open access policies or other institutional restrictions that conflict with any of the rights or provisions of this License, such Author has obtained the necessary waiver from his or her university or institution.

This License must be signed by the Author(s) and, in the case of a Work Made for Hire, also by the Copyright Owners. One Author/Copyright Owner may sign on behalf of all the contributors/owners only if they all have authorized the signing, approved of the License, and agreed to be bound by it. The signing Author and, in the case of a Work Made for Hire, the signing Copyright Owner warrants that he/she/it has full authority to enter into this License and to make the grants this License contains.

1. The Author must please sign here *(except* if an Author is a U.S. Government employee, then please sign under #3 below):

Karim Sultanov 24. 11. 2025

Author(s) Signature Print Name Date

2. The Copyright Owner (if different from the Author) must please sign here:

Name of Copyright Owner Authorized Signature and Title Date

3. If an Author is a U.S. Government employee, such Author must please sign below.
The signing Author certifies that the Work was written as part of his/her official duties and is therefore not eligible for copyright protection in the United States.

Name of U.S. Government Institution (e.g., Naval Research Laboratory, NIST)

Author Signature Print Name Date

PLEASE NOTE: NATIONAL LABORATORIES THAT ARE SPONSORED BY U.S. GOVERNMENT AGENCIES BUT ARE INDEPENDENTLY RUN ARE NOT CONSIDERED GOVERNMENT INSTITUTIONS. (For example, Argonne, Brookhaven, Lawrence Livermore, Sandia, and others.) Authors at these types of institutions should sign under #1 or #2 above.

If the Work was authored under a U.S. Government contract, and the U.S. Government wishes to retain for itself and others acting on its behalf, a paid-up, nonexclusive, irrevocable, worldwide license in the Work to reproduce, prepare derivative works from, distribute copies to the public, perform publicly, and display publicly, by or on behalf of the Government, please check the box below and add the relevant Contract numbers.

☐ Contract #(s) _____ [1.16.1]

LICENSE TERMS DEFINED

Accepted Manuscript (AM): The final version of an author's manuscript that has been accepted for publication and incorporates all the editorial changes made to the manuscript after submission and peer review. The AM does not yet reflect any of the publisher's enhancements to the work such as copyediting, pagination, and other standard formatting.

arXiv: An electronic archive and distribution server for research article preprints in the fields of physics, mathematics, computer science, quantitative biology, quantitative finance, and statistics, which is owned and operated by Cornell University, http://arxiv.org/.

Commercial and noncommercial scholarly use: *Noncommercial* scholarly uses are those that further the research process for authors and researchers on an individual basis for their own personal purposes. They are author-to-author interactions meant for the exchange of ideas. *Commercial* uses fall outside the author-to-author exchange and include but are not limited to the copying or distribution of an article, either in hard copy form or electronically, for resale or licensing to a third party; posting of the AM or VOR of an article by a site or service where an access fee is charged or which is supported by commercial paid advertising or sponsorship; use by a for-profit entity for any type of promotional purpose. Commercial uses require the permission of AIP Publishing.

Embargo period: The period of time during which free access to the full text of an article is delayed.

Employer's web page: A web page on an employer's site that highlights the accomplishments and research interests of the company's employees, which usually includes their publications. (See also: Personal web page and Scholarly Collaboration Network).

Exclusive License to Publish: An exclusive license to publish is a written agreement in which the copyright owner gives the publisher exclusivity over certain inherent rights associated with the copyright in the work. Those rights include the right to reproduce the work, to distribute copies of the work, to perform and display the work publicly, and to authorize others to do the same. The publisher does not hold the copyright to the work, which continues to reside with the author. The terms of the AIP Publishing License to Publish encourage authors to make full use of their work and help them to comply with requirements imposed by employers, institutions, and funders.

Full Credit Line: AIP Publishing's preferred format for a credit line is as follows (you will need to insert the specific citation information in place of the capital letters): "Reproduced from [FULL CITATION], with the permission of AIP Publishing." A FULL CITATION would appear as: Journal abbreviation, volume number, article ID number *or* page number (year). For example: Appl. Phys. Lett. 107, 021102 (2015).

Institutional repository: A university or research institution's digital collection of articles that have been authored by its staff and which are usually made publicly accessible. As authors are encouraged and sometimes required to include their published articles in their institution's repository, the majority of publishers allow for deposit of the Accepted Manuscript for this purpose. AIP Publishing also allows for the VOR to be deposited 12 months after publication of the Work.

Journal editorial office: The contact point for authors concerning matters related to the publication of their manuscripts. Contact information for the journal editorial offices may be found on the journal websites under the "About" tab.

Linking to the Version of Record (VOR): To create a link to your article in an AIP Publishing journal or proceedings, you need to know the CrossRef digital object identifier (doi). You can find the doi on the article's abstract page. For instructions on linking, please refer to our Web Posting Guidelines at https://publishing.aip.org/authors/web-posting-guidelines.

National Laboratories: National laboratories are sponsored and funded by the U.S. Government but have independent nonprofit affiliations and employ private sector resources. These institutions are classified as Federally Funded Research and Development Centers (FFRDCs). Authors working at FFRCs are not considered U.S. Government employees for the purposes of copyright. The Master Government List of FFRDCs may be found at http://www.nsf.gov/statistics/ffrdclist/.

Personal web page: A web page that is hosted by the author or the author's institution and is dedicated to the author's personal research interests and publication history. An author's profile page on a social media site or scholarly collaboration network site is *not* considered a personal web page. (See also: Scholarly Collaboration Network; Employer's web page).

Peer X-Press: A web-based manuscript submission system by which authors submit their manuscripts to AIP Publishing for publication, communicate with the editorial offices, and track the status of their submissions. The Peer X-Press system provides a fully electronic means of completing the License to Publish. A hard copy of the Agreement will be supplied by the editorial office if the author is unable to complete the electronic version of the form. (Conference Proceedings authors will continue to submit their manuscripts and forms directly to the Conference Editors.)

Preprint: A version of an author's manuscript intended for publication but that has not been peer reviewed and does not reflect any editorial input or publisher enhancements.

Professional Publication Ethics: AIP Publishing provides information on what it expects from authors in its "Statement of ethics and responsibilities of authors submitting to AIP Publishing journals" (http://publishing.aip.org/authors/ethics). AIP Publishing is also a member of the Committee on Publication Ethics (COPE) (http://publicationethics.org/), which provides numerous resources and guidelines for authors, editors, and publishers with regard to ethical standards and accepted practices in scientific publishing.

Scholarly Collaboration Network (SCN): Professional networking sites that facilitate collaboration among researchers as well as the sharing of data, results, and publications. SCNs include sites such as Academia.edu, ResearchGate, and Mendeley, among others.

Supplementary Material: Related material that has been judged by peer review as being relevant to the understanding of the article but that may be too lengthy or of too limited interest for inclusion in the article itself. Supplementary Material may include data tables or sets, appendixes, movie or audio clips, or other multimedia files.

U.S. Government employees: Authors working at Government organizations who author works as part of their official duties and who are not able to license rights to the Work, since no copyright exists. Government works are in the public domain within the United States.

Version of Record (VOR): The final published version of the article as it appears in the printed journal/proceedings or on the Scitation website. It incorporates all editorial input, is formatted in the publisher's standard style, and is usually viewed in PDF form.

Waiver: A request made to a university or institution to exempt an article from its open-access policy requirements. For example, a conflict will exist with any policy that requires the author to grant a nonexclusive license to the university or institution that enables it to license the Work to others. In all such cases, the Author must obtain a waiver, which shall be included in the manuscript file.

Work: The "Work" is considered all the material that comprises the article, including but not limited to the abstract, tables, figures, images, multimedia files that are directly embedded within the text, and the text itself. The Work does not include the Supplementary Material (see Supplementary Material above).

Work Made for Hire: Under copyright law, a work prepared by an employee within the scope of employment, or a work that has been specially ordered or commissioned for which the parties have agreed in writing to consider as a Work Made for Hire. The hiring party or employer is considered the author and owner of the copyright, not the person who creates the work.